



1.0 Overview and Science Justification

Jared Males, Laird Close and the MagAO-X Team

1 Introduction

AO systems are now in routine use at many telescopes in the world; however, nearly all work only in the infrared (IR, $\lambda > 1 \mu\text{m}$) due to the challenges of working at shorter wavelengths. The Magellan AO (MagAO) system was the first to routinely produce visible-AO science on a large aperture telescope. In Figure 1, we show an example of the power of large diameter visible-AO. Other large telescopes with visible AO systems include the 5 m at Palomar (Dekany et al., 2013) and ESO’s 8 m VLT with the ZIMPOL camera behind the Spectro-Polarimetric High-contrast Exoplanet REsearch (SPHERE) (Roelfsema et al., 2014).

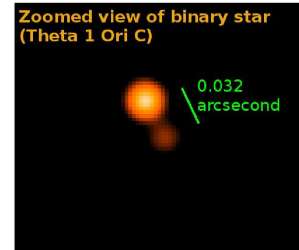


Figure 1: MagAO/VisAO r' image of the 32 mas binary θ^1 Ori C (Close et al., 2013).

MagAO-X is a *new* visible-to-near-IR “extreme” AO (ExAO) system. When completed, MagAO-X will consist of: (1) 2048 high-order actuators controlled at (up to) 3.7 kHz; (2) cutting-edge coronagraphs to block a star’s light; and (3) a suite of focal plane instruments including imagers and spectrographs enabling high-contrast and high-resolution science.

MagAO-X will deliver high Strehls ($\gtrsim 70\%$ at $H\alpha$), high resolutions (14–30 mas), and high contrasts ($\lesssim 10^{-4}$) from ~ 1 to $10 \lambda/D$. Among many compelling science cases, MagAO-X will revolutionize our understanding of the earliest stages of planet formation, enable high spectral-resolution imaging of stellar surfaces, and could take the first images of an exoplanet in reflected light.

1.1 Existing MagAO and 2000 Hz: Our current MagAO system combines a second-generation 585 actuator adaptive secondary mirror (ASM) and a cutting-edge pyramid wavefront sensor (PWFS). MagAO is mounted on the 6.5 m Magellan Clay telescope at Las Campanas Observatory (LCO), Chile. MagAO has two science cameras, namely the Clio IR camera (1–5 μm) (Morzinski et al., 2015) and VisAO (0.6–1 μm). The combination of fine spatial sampling (300 to 400 modes), up to 2 kHz speed, the excellent site, and the ASM and PWFS has enabled—for the first time—filled-aperture, diffraction-limited imaging at visible wavelengths on a large telescope: at wavelengths as blue as r' ($\lambda_0 = 624\text{nm}$, Fig. 1).

We have recently completed an upgrade of the existing MagAO system, improving the loop speed from 1000 Hz to 2000 Hz. In 0.6” to 0.7” seeing (somewhat worse than median at LCO), we measured the improvement in z' (0.9 μm) image quality. The results are shown in Figure 2. These results show the benefits of increased AO loop speed.

1.2 Introduction to MagAO-X: MagAO-X will be an ExAO system optimized for working in the optical ($\lambda < 1 \mu\text{m}$) while (eventually) providing imaging and spectroscopic capabilities out to H band (1.6 μm). In its final form, it will consist of a 2000 actuator Boston Micromachines Corp. (BMC) deformable mirror (DM) controlled by a PyWFS operating at up to 3.63 kHz. Diffracted starlight will be suppressed using coronagraphs, and using techniques such as Low-order and focal-plane wavefront sensing (LOWFS and FPWFS) in real-time



MagAO-X Preliminary Design
1.0 Overview and Science Justification

Doc #:	MagAOX-001
Date:	2017-04-24
Status:	Rev. 0.0
Page:	2 of 9

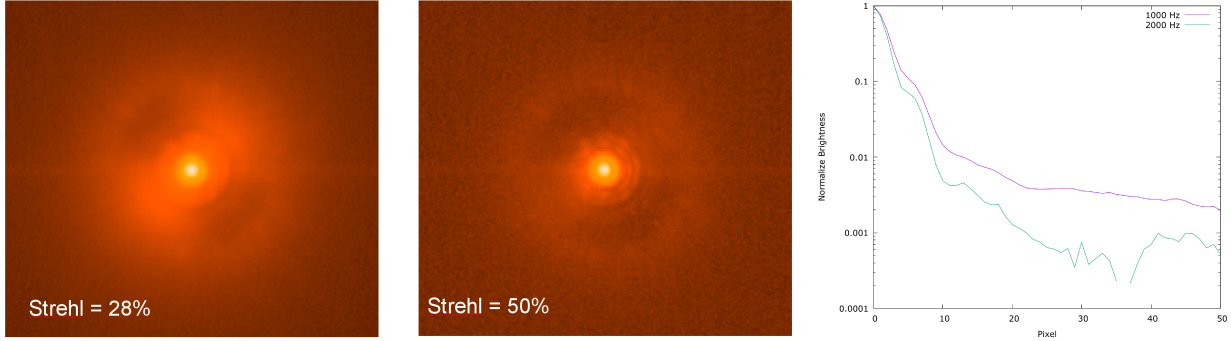


Figure 2: The benefits of speed. Here we show the improvement realized when speeding the existing MagAO system up from 1 kHz to 2 kHz. The PSF images are for z' ($0.9 \mu\text{m}$) in slightly worse than median conditions at LCO ($0.7''$ seeing) on a cloudy night. The improvement in Strehl is obvious. The cuts plotted at right show the improvement in the full-width at half maximum and dark hole contrast (even without a coronagraph).

the impact of static and non-common path (NCP) aberrations will be minimized. Finally, we make use of post-processing techniques such as simultaneous differential imaging and angular differential imaging to achieve the highest possible contrasts.

We have organized MagAO-X into 3 phases. This approach will allow us to manage the complexity and risk more effectively than possible if the entire instrument were delivered at once. It also more efficiently uses telescope allocations during commissioning, as it provides time to analyze critical on-sky results and re-optimize the instrument between runs. Each of the three phases will be scientifically productive, ensuring that the MagAO-X project will have a *major science impact early on* while we build to our ultimate scientific goals.

NOTE: only Phase I and Phase II are the subjects of this PDR. Phase III is described here for context, but we are deferring preliminary design of the final phase to a future effort.

Briefly, the three phases are:

Phase I: A new visible-wavelength vector apodizing phase plate (vAPP) coronagraph, optimized for $H\alpha$, will be introduced. We will exploit the vAPP leakage term (explained in detail below) to perform LOWFS. This phase will employ the main optical train of MagAO-X, but use the *existing* MagAO system for high-order wavefront control without using the new MEMS DM. While this will provide only moderate Strehl ratio to the coronagraphic system, it will still be an advance over existing MagAO+VisAO, which has no diffraction-rejecting coronagraphic capabilities. The LOWFS will employ offloading to the Pyramid via slope offsets, a standard technique for the LBT/MagAO architecture. Importantly, this phase will provide an on-sky test of the optical train, and test the vAPP LOWFS on-sky. We will also perform a fit and alignment check of the $f/11$ feed using our on-board woofer (in preparation for Phase II).

Science focal plane instrumentation will initially include two electron multiplying CCDs (EMCCD) for $\lambda \lesssim 1 \mu\text{m}$, with $J-H$ bands ($1.2-1.6 \mu\text{m}$) being sensed by our existing Clio camera. This capability will allow initial observations in the MaXProtoPlanets survey (described below) on the brightest targets where existing MagAO achieves moderately good correction at $H\alpha$.

By getting the basic instrument on-sky at the telescope as early as possible, we will retire risk associated with the optics design and layout, the coronagraph architecture, the LOWFS strategy (crucial for rejecting instrumental

	MagAO-X Preliminary Design 1.0 Overview and Science Justification	Doc #: MagAOX-001 Date: 2017-04-24 Status: Rev. 0.0 Page: 3 of 9
---	--	---

quasi-static speckles at small separations), and our shipping and handling plan. This phase will be scientifically productive, kicking off one of our major science projects.

Phase II: The main new goal of the second phase is to bring the new high-order (HO) wavefront control system on-line. This will consist of a new woofer (an Alpao DM97) and a new tweeter (a Boston Micromachines 2k), along with a new PWFS using an OCAM-2K EMCCD camera. This new hardware will be integrated with the coronagraph, which will now be fed with wavefronts having Strehl ratios of $\sim 70\%$ at $H\alpha$ on brighter guide stars. Significantly, this will allow high contrast imaging on guide stars as faint as 12th mag. This then enables the MaXProtoPlanets survey, a census of low-mass accreting proto-planets around all of the T Tauri and Herbig Ae/Be stars accessible from LCO.

The initial development and testing for Phase II will be conducted in the ExAO and Coronagraphy lab on a separate optical bench. This will enable Phase II to start in parallel with the later stages of Phase I. Once Phase I is complete and the instrument has been shipped back to Steward, the new hardware will be integrated on the MagAO-X bench.

It is during this phase of the project that we will begin the MaXProtoPlanets survey in earnest.

Phase III: In the final phase of the project we will introduce a new coronagraph and spectrographic capabilities. The phase induced amplitude apodization complex-mask coronagraph (PIAACMC) and lyot-based LOWFS will be integrated in the system. The PIAACMC is capable of achieving a high throughput design (say 78% off-axis) small IWA $< 1\lambda/D$, over a broad 20% bandpass on a complex aperture (including spiders, etc.) Here we will also employ an energy-resolving microwave kinetic inductance detector (MKID) array, which provides integral field spectroscopy (IFS) from 0.7–1.4 μm . An important goal of this instrument is to use the MKIDS as FPWFS to achieve the highest possible speckle suppression. Finally, “RHEA@MagAO-X” a 9-element, visible light, single-mode fiber, $R \sim 60,000$ spectrograph will be used for high spatial and spectral resolution science behind MagAO-X. As noted above, the preliminary design of Phase III is not being presented here.

2 Science Justification

For the purposes of this review, we are focusing on one main science case: a survey of nearby T Tauri and Herbig Ae/Be stars for newly formed accreting planets in $H\alpha$. We describe this science case in the following section and present the high level performance requirements we derive from it.

2.1 A Survey of the Low Mass Distribution of Young Gas Giant Planets: We now know that wide (>30 AU) massive ($>4 M_{Jup}$) giant planets (EGPs) are rare (e.g. Biller et al., 2013). Yet there are hints of a major population of lower mass ($0.5\text{--}2 M_{Jup}$) EGP’s closer in, from $\sim 5\text{--}20$ AU (Sallum et al., 2015). Such EGP’s may well determine the delivery of volatiles to potentially habitable inner terrestrial planets (Raymond et al., 2004; Matsumura et al., 2015). A key goal of the decadal Astro2010 survey is the *characterization of habitable planets*, as well as understanding planet formation. MagAO-X will image protoplanets in $H\alpha$ (for H recombination $H\alpha$ is $\sim 1760\%$ stronger than the best near-IR line Pa β) in the luminous accretion phase of formation to address these goals (not possible with GPI’s IR IFS).

2.1.1 Proof-of-concept – Imaging LkCa 15 b at $H\alpha$: We used MagAO’s simultaneous differential imaging (SDI) mode (Close et al., 2014) to discover $H\alpha$ from a forming protoplanet (LkCa 15 b) for the first time (Sallum et al., 2015) (see Fig. 3), detecting an accretion stream shock from a 90 mas (15 AU) protoplanet. Dynamical stability places the mass of LkCa 15 b at $2_{-1.5}^{+3} M_{Jup}$. Correcting for extinction we found an accretion rate of $\dot{M} = 1.16 \times 10^{-9} M_{\odot}/\text{yr}$ (Sallum et al., 2015). Observed $H\alpha$ rate was $\sim 0.5e/s$ at the peak pixel at Strehl $\sim 5\%$.

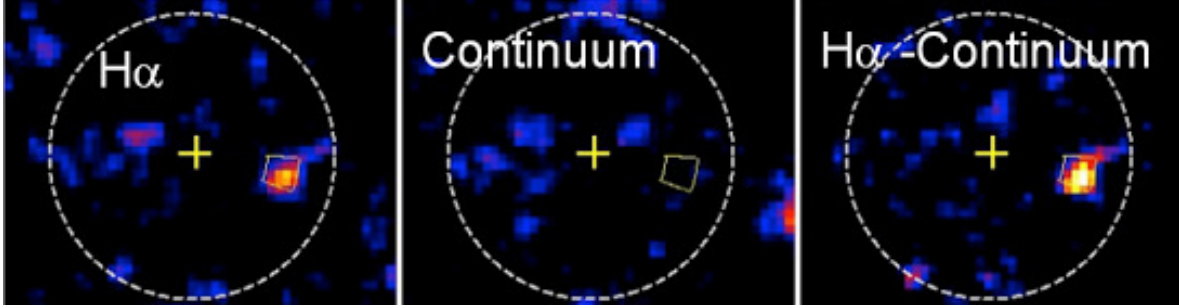


Figure 3: LkCa 15 b, a protoplanet imaged with SDI at $H\alpha$. Sallum et al. 2015.

2.1.2 MagAO-X $H\alpha$ Protoplanet Survey (MaXProtoPlanetS): While LkCa 15 (145 pc; 1–2 Myr) is fairly faint ($I \sim 11$ mag) there are many brighter, closer similarly young accreting targets. In the η Cha (Mamajek et al., 1999), ϵ Cha (Murphy et al., 2013), ρ Oph (Luhman & Rieke, 1999), TW Hya (Mamajek, 2005), and Upper Sco (de Zeeuw et al., 1999) clusters, which are all < 5 –10 Myr old within $\lesssim 150$ pc, there are ***exactly 160 individually vetted accreting targets with $I \leq 10$ mag***. These are good guide stars for Phase I of MagAO-X. Around all these target stars a planet like LkCa 15 b would be at ~ 100 –200 mas separations (~ 15 AU), but instead of $\Delta H\alpha = 5.3$ mag it could (conservatively) be 5 mag fainter still — due to extra dust extinction (no disk gaps like LkCa 15), and/or lower mass of the planet. The worst case $\Delta H\alpha \sim 11$ mag contrast is too high for the *existing* MagAO but will be achievable with MagAO-X. Utilizing MagAO-X’s SDI+vAPP mode, we will observe the $H\alpha/H\beta$ line ratio that can be compared to Case-B recombination theory (Hummer & Storey, 1987); hence, the line of sight extinction (A_R) can be estimated (Close et al., 1997). As a result, the true $H\alpha$ line strength can be measured and protoplanet masses estimated (Close et al., 2014), see Fig. 4. An $I = 10$ mag star in median conditions with a $0.5 M_{Jup}$ EGP and 2.5 mag greater A_R and the same \dot{M} as LkCa 15b ($\Delta H\alpha = 10.3$ mag) will have peak pixel S/N ~ 11 in 2 hrs with our KLIP (Soummer et al., 2012) pipeline (accounting for EMCCD excess noise, MagAO-X+vAPP throughput, Strehl and contrast).

There are six (2 of spectral type A and 4K spectral types) $I < 10$ mag targets in the η Cha cluster (50 pc, ~ 10 Myr) (Mamajek et al., 1999), 15 $I < 10$ targets (1B, 4A, 2G, and 8K SpT) in the ϵ Cha cluster (100 pc, 3 – 5 Myr) (Murphy et al., 2013), two $I < 10$ targets (1B and 1A SpT) in the ρ Oph cluster (140 pc, 1 Myr) (Luhman & Rieke, 1999), 17 $I < 10$ targets (2A, 3K, and 12M SpT) in the TW Hya cluster (50 pc, ~ 10 Myr) (Mamajek, 2005), and finally an additional 120 $I < 10$ targets (49B, 34A, 22F, 9G, 4K, and 2M SpT) in the Upper Sco cluster (150 pc, 5–10 Myr) (de Zeeuw et al., 1999). **So there are a total of 160 < 10 Myr old accreting $D < 150$ pc targets all with $I < 10$ mag for the MaXProtoPlanets survey—all bright enough for good AO correction.** There are also many slightly fainter targets $I < 12$ mag that will be dis.

Extrapolating from our initial ($3/10 = 30\%$) success rate for the young star GAPplanetS $H\alpha$ survey having accreting objects (Follette et al., 2016) the 160 stars yield ~ 48 new protoplanet systems using just 5 nights per semester.

In Phase II we can achieve the same contrasts on fainter $I = 12$ stars which yields 33 more (ϵ Cha, ρ Oph) targets, yielding ~ 11 more detections—raising the total to ~ 59 systems. **MaXProtoPlanetS’s $\sim 59 \times$ larger sample of detected protoplanet systems will define the population of low-mass outer EGPs, and will help reveal where/how gas planets actually form and grow.** Integrating over the secure members of the above youngest

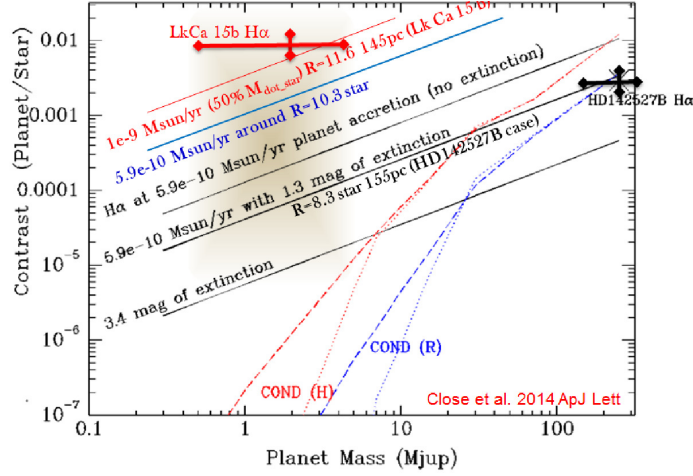


Figure 4: Relation between the mass of the $H\alpha$ planet to the observed contrast (as a function of M_{Rstar} , A_R , & \dot{M} of the planet).

clusters (ϵ Cha, ρ Oph) yields exactly 16 and 17 (respectively) more 1–3 Myr targets from $10 < I < 12$ mag. These 32 targets should yield another ~ 11 discoveries, raising the total to ~ 60 . ***This would increase the number of known protoplanets systems by $\sim 60\times$, define the population of low-mass outer EGPs, and for the very first time reveal where gas planets actually form.***

2.1.3 High Level Performance Requirements: From the MaXProtoPlanets survey we derive the high level performance requirements for MagAO-X. These are present in Table 1. The main requirement is to achieve the contrast at the given separation. This places requirements on WFC at specific spatial frequencies. Strehl ratio, which is a global image quality metric, is a “soft” requirement – we need high image quality but do not need to achieve an exact Strehl ratio so long as the contrast is achieved.

Table 1: The high level performance requirements derived from the MaXProtoPlanets $H\alpha$ SDI survey.

Targets			Performance		
I	d	Numb.	Sep	$\Delta H\alpha$	Strehl ¹
mag	[pc]		[mas]	mag	[%]
5	225	6	75	12.0	70
8	150	25	100	9.0	50
10	150	129	100	7.0	30
12	150	44 ²	100	5.0	20

¹ At $H\alpha$, $\lambda = 656$ nm.

² not complete, there are likely more

3 Other Science Cases

Here we present a short summary of several additional science cases. These are generally spanned by the parameters of the $H\alpha$ survey in terms of guide star brightness and separations, and are less-demanding, and so

	MagAO-X Preliminary Design 1.0 Overview and Science Justification	Doc #: MagAOX-001 Date: 2017-04-24 Status: Rev. 0.0 Page: 6 of 9
---	--	---

we do not specifically derive requirements for these. Rather, they are presented to give an idea of the breadth of use-cases for this new instrument.

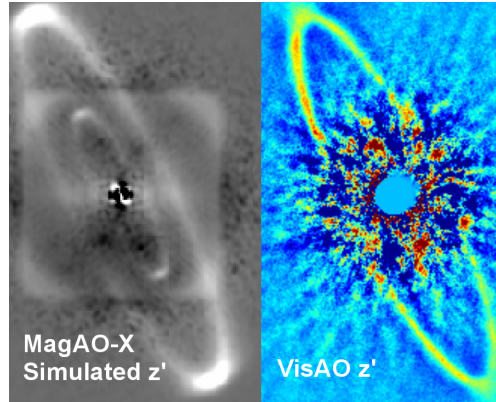


Figure 5: The HR 4796A disk. Left: simulated MagAO-X image at z' ($0.9 \mu\text{m}$) (includes hypothetical inner disk suggested by Rodigas et al. (2015)), just 5 seconds of data with simple PSF subtraction. Right: actual MagAO+VisAO image (Rodigas et al., 2015). MagAO-X will *significantly enhance our ability to probe the regions closest to the star*.

3.1 Circumstellar Disks: Disk science is a challenging application of AO, with low surface brightness and characteristics similar to the uncorrected seeing halo, so high-Strehl high-contrast ExAO is critical. MagAO-X will push the two frontiers in circumstellar disk science. The first is detailed imaging of geometry, particularly in the 5-50 AU region analogous to the outer part of the solar system. Most disks sit at 50-150 pc, so reaching radii comparable to the giant planet region requires imaging at 50-120 mas. Existing systems push in to at best ~ 150 mas. For some disks, an inner working angle of ~ 100 mas will push to the exozodiacal light region for the first time. For example, in the well-known HR 4796A disk, SED fits show that the $8\text{-}20 \mu\text{m}$ flux cannot be fully explained by the outer, ~ 100 K, ring, suggesting a ring at 3-7 AU (Wahhaj et al., 2005). MagAO-X has the potential to image this inner ring. The second frontier is multiwavelength study of disks to derive the chemical make-up and dynamical state (Rodigas et al., 2015; Stark et al., 2014). This requires a large wavelength grasp from visible through near-infrared so MagAO-X's ability to image at $\sim 0.45 \mu\text{m}$ complements existing systems.

3.2 Fundamental Properties of Young Solar-System-like EGPs: Dedicated exoplanet-imagers GPI and SPHERE are now operational, and GPI has discovered the first planet of this new era: 51 Eri b is a $600\text{-K } \sim 2 M_{\text{Jup}}$ exoplanet imaged 13 AU from its 20-Myr-old, 30-pc-away F-type host star (Macintosh et al., 2015). This planet is different from other exoplanets (whether imaged or analyzed by transit spectroscopy): its atmosphere is the closest analog yet to solar system atmospheres because of its Saturn-scale orbit, Jupiter-scale mass, and cool temperature such that CH_4 was detected in the GPI spectrum.

We have conducted a prototype experiment with existing MagAO using the exoplanet β Pic b, which can be imaged with the current VisAO due to its brightness (youth and mass) and its 300-400 mas separation. Fig. 6 shows images of β Pic b taken with the MagAO+VisAO camera (Males et al., 2014). Fig. 7 demonstrates using such measurements to empirically measure the fundamental properties of this solar-system-scale exoplanet—the luminosity of β Pic b (Morzinski et al., 2015). ***MagAO-X will extend these observations to shorter wavelengths, and to smaller mass, smaller separation planets such as 51 Eri b.*** MagAO-X will also enable characterization of such planets with the DARKNESS and RHEA@MagAO-X spectrographs.

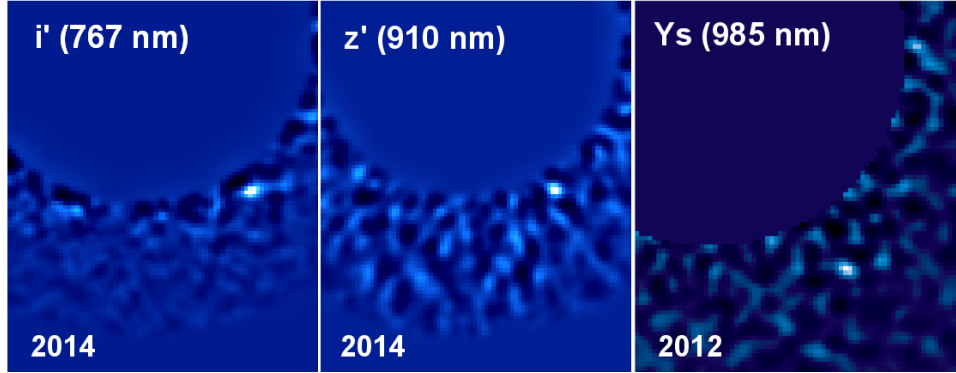


Figure 6: The exoplanet β Pic b imaged with VisAO, in i' & z' (Males et al, in prep) and Y_s (separation 470 mas, $\Delta Y_s=11.97$ mag, Males et al., 2014). MagAO-X will extend these observations to shorter wavelengths, and fainter, smaller-separation planets such as 51 Eri b.

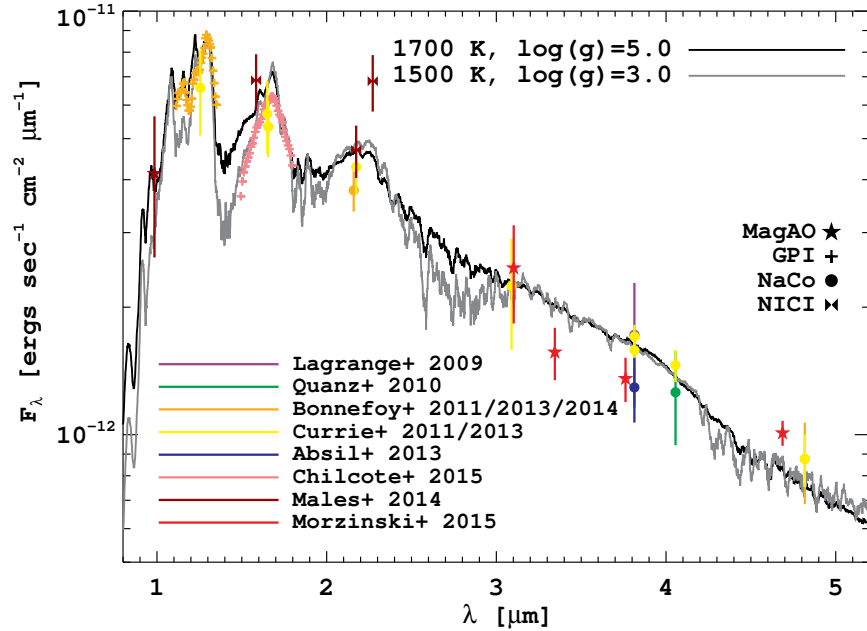


Figure 7: SED of young super-Jupiter β Pic b, with which we measured its bolometric luminosity, empirically for the first time (Morzinski et al., 2015). Plotted black and gray lines are degenerate BT Settl models with identical fits but different temperatures and gravities. MagAO-X will measure the Wien's slope in the visible to give the temperature for this and other young EGPs.

3.3 Resolved Stellar Photospheres: The 3x3 single-mode fiber-fed IFS, RHEA@MagAO-X, with $R \sim 60,000$ spectral resolution, will be provided by collaborator Mike Ireland. The combination of the ExAO resolution and contrast with high spectral resolution enables many exciting science cases. For instance: the largest resolvable non-Mira stars accessible from MagAO include Betelgeuse (~ 50 mas), Antares (~ 40 mas), Arcturus (~ 21 mas), Aldebaran (~ 20 mas) and α Boo (~ 19 mas). These stars lose mass through a complex process in an interplay between a hot ($\sim 10,000$ K) corona and a cool (~ 2000 K), slow (~ 10 km/s) molecular wind. These states can

	MagAO-X Preliminary Design 1.0 Overview and Science Justification	Doc #: MagAOX-001 Date: 2017-04-24 Status: Rev. 0.0 Page: 8 of 9
---	--	---

not co-exist so asymmetries of some kind are expected. Resolving the photosphere in lines and molecular bands enables the multi-dimensional structure of these regions to be imaged. Upwelling and downwelling velocities on the surface are of order a few km/s, separable at sufficient resolution. A single image of a stellar photosphere would be the *first ever direct measurement of convection in a star other than the Sun*.

3.4 Asteroids: MagAO-X will have resolutions of 14–21 mas in $g-r$ bands, which correspond to $\sim 20\text{--}30$ km on a main-belt asteroid (MBA). On a typical night more than 80 MBAs brighter than $I=13$ (implying $\gtrsim 50$ mas) will be resolvable by MagAO-X. This will provide true dimensions, avoiding degeneracies in light-curve analysis. MagAO-X will enable sensitive searches for and orbit determination of MBA satellites. In combination, these directly measure density and hence estimate composition (Britt et al., 2002). This will directly inform the theories of terrestrial planet formation (Mordasini et al., 2011).

4 Preliminary Design Review

The MagAO-X team has completed our preliminary designs of the following items:

- The optical design of Phase I and II
- Optical component specifications
- The mechanical design of Phase I and II
- The electronics design
- The shipping and handling plan
- The real-time and control software design
- The data management plan
- Wavefront control plan (as described with simulations)
- Management plan

Each of these areas are addressed in detail in the following sections, with specific requirements the designs are intended to meet.

References

- Biller, B. A., Liu, M. C., Wahhaj, Z., et al. 2013, ApJ, 777, 160
- Britt, D. T., Yeomans, D., Housen, K., & Consolmagno, G. 2002, Asteroids III, 485
- Close, L. M., Roddier, F., Hora, J. L., et al. 1997, ApJ, 489, 210
- Close, L. M., Males, J. R., Morzinski, K., et al. 2013, ApJ, 774, 94
- Close, L. M., Follette, K. B., Males, J. R., et al. 2014, ApJL, 781, L30
- de Zeeuw, P. T., Hoogerwerf, R., de Bruijne, J. H. J., Brown, A. G. A., & Blaauw, A. 1999, AJ, 117, 354

	MagAO-X Preliminary Design 1.0 Overview and Science Justification	Doc #: MagAOX-001 Date: 2017-04-24 Status: Rev. 0.0 Page: 9 of 9
---	--	---

- Dekany, R., Roberts, J., Burruss, R., et al. 2013, *ApJ*, 776, 130
- Follette, K. B., Miller Close, L., Males, J., et al. 2016, in American Astronomical Society Meeting Abstracts, Vol. 227, American Astronomical Society Meeting Abstracts, #106.05
- Hummer, D. G., & Storey, P. J. 1987, *MNRAS*, 224, 801
- Luhman, K. L., & Rieke, G. H. 1999, *ApJ*, 525, 440
- Macintosh, B., Graham, J. R., Barman, T., et al. 2015, *Science*, 350, 64
- Males, J. R., Close, L. M., Morzinski, K. M., et al. 2014, *ApJ*, 786, 32
- Mamajek, E. E. 2005, *ApJ*, 634, 1385
- Mamajek, E. E., Lawson, W. A., & Feigelson, E. D. 1999, *ApJL*, 516, L77
- Matsumura, S., Brasser, R., & Ida, S. 2015, *ArXiv e-prints*, 1512.08182
- Mordasini, C., Alibert, Y., Klahr, H., & Benz, W. 2011, in *European Physical Journal Web of Conferences*, Vol. 11, *European Physical Journal Web of Conferences*, 04001
- Morzinski, K. M., Males, J. R., Skemer, A. J., et al. 2015, *ApJ*, 815, 108
- Murphy, S. J., Lawson, W. A., & Bessell, M. S. 2013, *MNRAS*, 435, 1325
- Raymond, S. N., Quinn, T., & Lunine, J. I. 2004, *Icarus*, 168, 1
- Rodigas, T. J., Stark, C. C., Weinberger, A., et al. 2015, *ApJ*, 798, 96
- Roelfsema, R., Bazzon, A., Schmid, H. M., et al. 2014, *Proc. SPIE*, 9147, 91473W
- Sallum, S., Follette, K. B., Eisner, J. A., et al. 2015, *Nature*, 527, 342
- Soummer, R., Pueyo, L., & Larkin, J. 2012, *ApJL*, 755, L28
- Stark, C. C., Schneider, G., Weinberger, A. J., et al. 2014, *ApJ*, 789, 58
- Wahhaj, Z., Koerner, D. W., Backman, D. E., et al. 2005, *ApJ*, 618, 385